

Quality of Mass-Produced Lead Tungstate Crystals

Rihua Mao, Liyuan Zhang, *Member, IEEE*, and Ren-Yuan Zhu, *Senior Member, IEEE*

Abstract—Because of the broad interest in high energy and nuclear physics community, mass production capacities of lead tungstate crystals have been established. The optical and scintillation properties of lead tungstate crystals, 20 each from two major vendors, were evaluated. The transmittance, emission and excitation spectra, light output and light response uniformity of these samples were measured. The degradations of these properties under irradiation, and the emission weighted radiation induced absorption coefficient (*EWRIAC*) were also studied. It was found that currently mass-produced lead tungstate crystals are radiation hard enough for radiation environments where expected dose rates do not exceed a few hundred rad/h.

Index Terms—Crystal, emission, lead tungstate, light output, radiation damage, scintillator, transmission.

I. INTRODUCTION

LEAD tungstate (PbWO_4 or PWO) crystal is a heavy scintillator with high density (8.3 g/cm^3), short radiation length (0.89 cm) and small Molière radius (2.2 cm). Yttrium doped PbWO_4 crystals have an emission spectrum peaked at 420 nm with FWHM of 120 nm [1]. After extensive R&D, PWO crystals are now in mass production. A few tens of thousands crystals have been produced at Bogoroditsk Techno-Chemical Plant (BTCP) in Tula, Russia, for the CMS experiment at CERN [2]. Shanghai Institute of Ceramics (SIC) in Shanghai, China, has produced a few thousand crystals for the PrimEx experiment at Jefferson laboratory [3]. Two batches of PWO crystals, 20 each randomly selected from mass produced crystals, were evaluated at Caltech. BTCP samples have tapered shape: $30 \times 30 \text{ mm}^2$ at the large end, $28.5 \times 28.5 \text{ mm}^2$ at the small end and 220 mm long. SIC samples are rectangular with a dimension of $22 \times 22 \times 230 \text{ mm}^3$. Fig. 1 shows typical samples from BTCP and SIC.

All surfaces of these samples are polished. It is interesting to note that BTCP PWO crystals are triple doped with lanthanum, yttrium and niobium [4], and are grown along the “*a*” axis by the Czochralski method [1]. SIC PWO crystals, however, are single doped with yttrium only and are grown along the “*c*” axis by a modified Bridgman method [1].

All samples were first annealed at $200 \text{ }^\circ\text{C}$ for 4 h to remove any residual radiation induced absorption and to restore the sample to its initial state [5], [6]. After annealing, samples were kept in dark at $18 \text{ }^\circ\text{C}$ for at least 48 h before initial measurement. It was found that PWO optical properties are stable after 8 h of thermal annealing. All samples also went through γ -ray irradiations at 15 400 and 9000 rad/h until reaching an

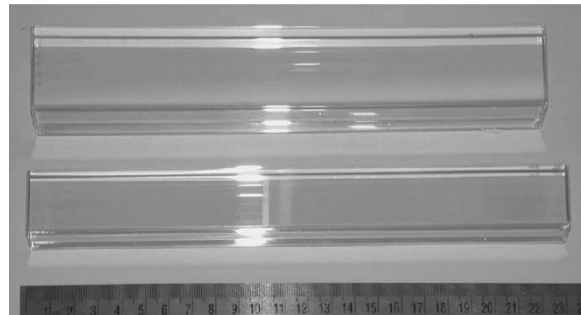


Fig. 1. Typical BTCP (top) and SIC (bottom) PWO samples.

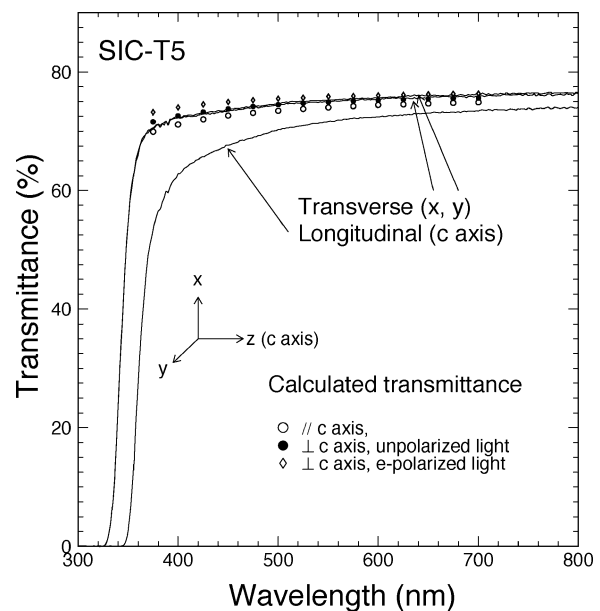


Fig. 2. Initial longitudinal and transverse transmittance spectra are shown as function of wavelength for sample SIC-T5.

equilibrium [7]. Optical and scintillation properties before and after irradiations were measured.

II. INITIAL OPTICAL AND SCINTILLATION PROPERTIES

Longitudinal transmittance was measured by using a Hitachi U-3210 UV/visible spectrophotometer with double beam, double monochromator and a large sample compartment equipped with a custom Halon coated integrating sphere. The systematic uncertainty in repeated measurements is about 0.2%.

Figs. 2 and 3 show typical initial longitudinal and transverse transmittance spectra for samples from SIC and BTCP respectively. Also shown in these figures are the theoretical limits of the transmittance assuming no internal absorption, calculated by using the refractive index of the “ordinary” light, which propagates along the “*c*” axis and has a polarization perpendicular

Manuscript received October 31, 2003. This work was supported in part by the U.S. Department of Energy Grant DE-FG03-92-ER40701.

The authors are with the California Institute of Technology, Pasadena, CA 91101 USA (e-mail: zhu@hep.caltech.edu).

Digital Object Identifier 10.1109/TNS.2004.832561

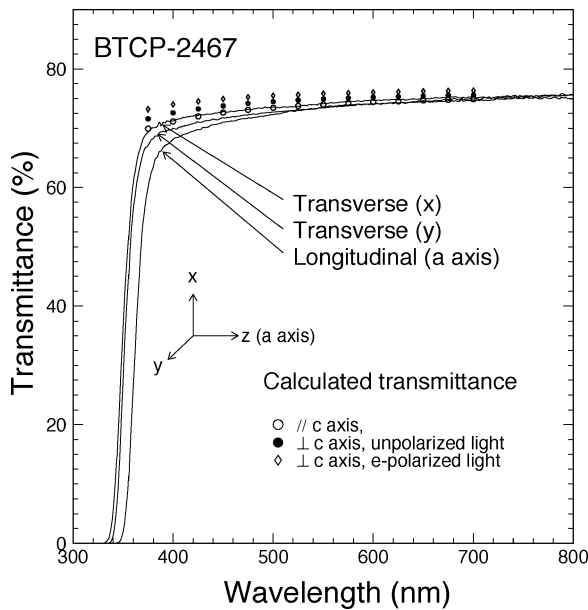


Fig. 3. Initial longitudinal and transverse transmittance spectra are shown as function of wavelength for sample BTCP-2467.

to the “*c*” axis, the “extraordinary” light, which propagates perpendicular to the “*c*” axis and has a polarization along the “*c*” axis, and unpolarized light which propagates perpendicular to the “*c*” axis [5], [8], [9]. Because of the birefringence, the theoretical transmittance limit of the “extraordinary” light is about 3% higher than that of the “ordinary” light at PWO emission peak. Chinese crystals are grown along the “*c*” axis, so its longitudinal transmittance should be compared to the theoretical limit for light propagation along the “*c*” axis and independent of polarization. Russian crystals are grown along the “*a*” axis, so its theoretical limit of longitudinal transmittance is a combination of the refractive indexes of the “ordinary” and the “extraordinary” components. Both Russian and Chinese crystals approach the theoretical limit, indicating very low intrinsic absorption.

Fig. 4 shows a comparison of initial longitudinal transmittance at 440 nm, which is the primary wavelength adapted by the CMS ECAL collaboration to monitor PWO crystal calorimeter [10]. The average transmittance at 440 nm is 70% with normalized rms spreads of 1.4% for the BTCP samples. The corresponding values for the SIC samples are 66% and 1.5%, respectively. Compared to the BTCP samples, the SIC samples have 4.2% lower transmittance. Part of this difference may be explained by the birefringent nature of PWO crystals, since the theoretical transmittance without absorption is about 3% higher if measured along the “*a*” axis as compared to the “*c*” axis.

The blue scintillation of yttrium doped PWO crystals has a fast decay time. The scintillation light output and decay kinetics were measured using a Hamamatsu PMT R2059, which has a bi-alkali photo cathode and a quartz window. For measurements of the light output the large end of a sample was coupled to the PMT with Dow Corning 200 fluid, while all other faces of the sample were wrapped with Tyvek paper. A collimated ^{137}Cs source was used to excite the sample. The γ -ray peak was obtained by a simple Gaussian fit, and was used to determine photoelectron numbers by using calibrations of

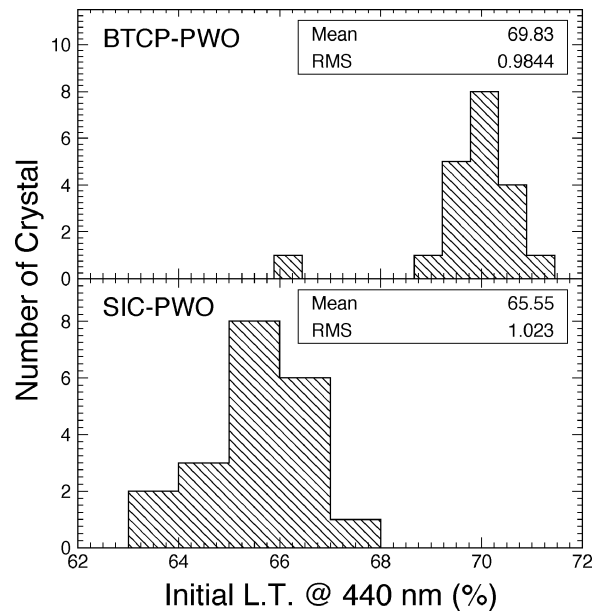


Fig. 4. A comparison of initial longitudinal transmittance at 440 nm.

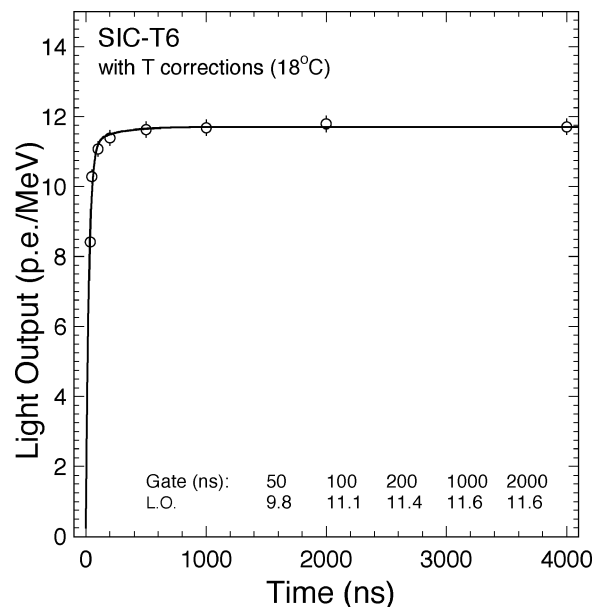


Fig. 5. Initial light output is shown as function of integration time for sample SIC-T6.

the single photo electron peak. The measured values of light output was corrected to 18 °C by using temperature coefficient of $-1.98\%/^{\circ}\text{C}$. The light output of a samples is defined as an average of nine data points obtained by shooting the γ -ray source at nine evenly distributed locations along the long crystal side. The systematic uncertainty of light output measurement thus is reduced to less than 1% [1].

Figs. 5 and 6 show typical initial light output as a function of integration time. Data in these figures are in units of number of photo electrons per MeV of energy deposition (p.e./MeV). PWO crystals from both BTCP and SIC have fast decay time. The ratio of light output integrated between 50 and 100 ns to 1 μs is 82% and 96%, respectively, for the BTCP samples. The corresponding numbers are 83% and 96% for the SIC samples.

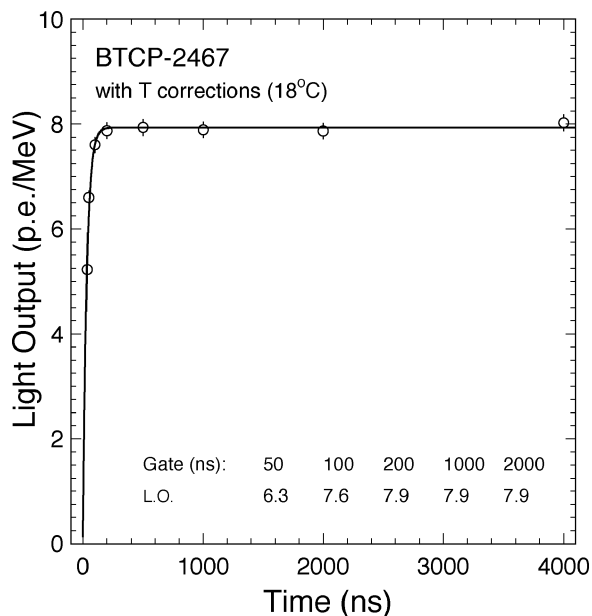


Fig. 6. Initial light output is shown as function of integration time for sample BTCP-2467.

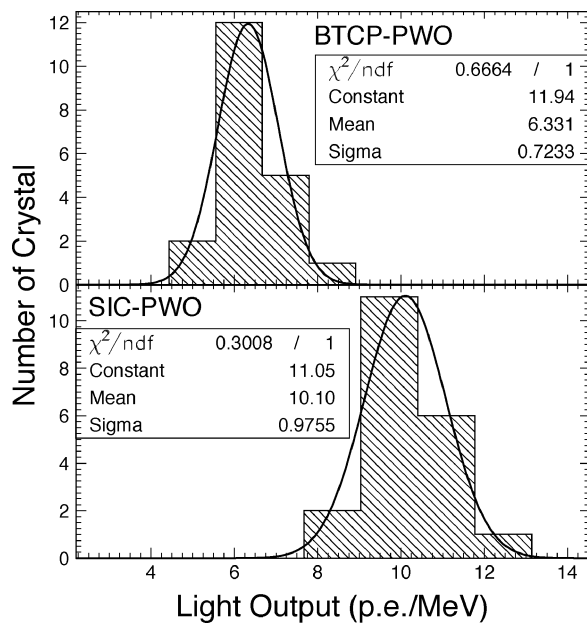


Fig. 7. A comparison of initial light output.

Fig. 7 shows distributions of the light output integrated over 200 ns. The average light output for the BTCP samples is 6.4 p.e./MeV with normalized rms spreads of 12%. The corresponding numbers for the SIC samples are 10 p.e./MeV and 9.6%. The light output of the SIC samples is 58% higher than that from the BTCP. This large difference can not be explained by crystal geometry since the slimmer and longer SIC samples are supposed to have lower light collection efficiency as compared to the BTCP samples. The excessive (130–280 ppmw) lanthanum doping in PWO crystals produced at BTCP [4], however, is suspected to suppress the light output. Further investigation will be carried out to clarify this issue.

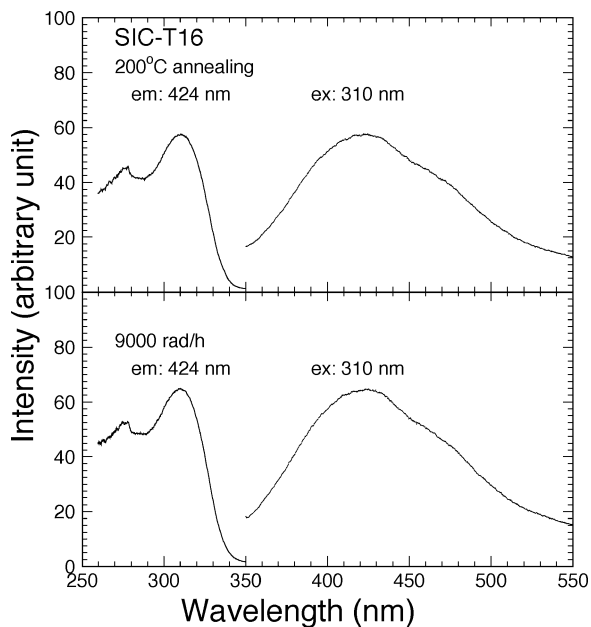


Fig. 8. Excitation and photoluminescence spectra are shown before and after γ -ray irradiations at 9000 rad/h for sample SIC-T25.

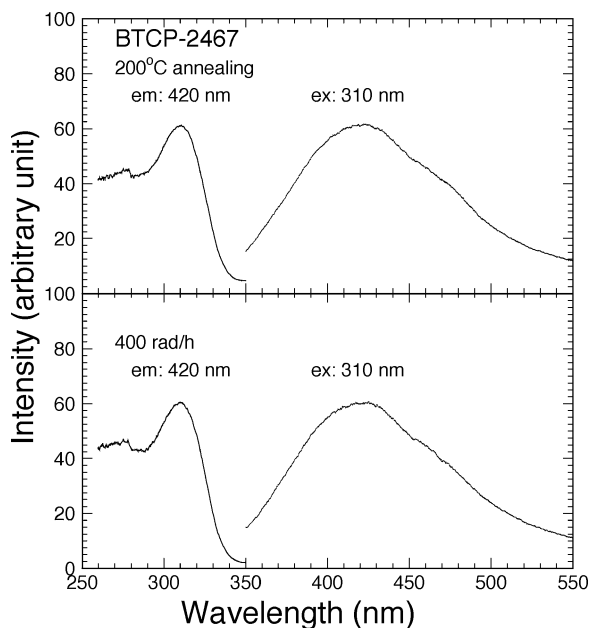


Fig. 9. Excitation and photoluminescence spectra are shown before and after γ -ray irradiations at 400 rad/h for sample BTCP-2467.

III. RADIATION DAMAGE

Over the last seven years, we learned that the PWO scintillation mechanism is not affected by γ -ray irradiations, the loss of light output is due only to radiation induced absorption caused by color center formation, and it is dose rate dependent [7].

Photo luminescence was measured by using a Hitachi F-4500 fluorescence spectrophotometer, where UV excitation light was shot to a bare surface of the sample and photo luminescence, without passing through sample, was measured by a photo multiplier tube (PMT) through a monochromator.

Figs. 8 and 9 show the excitation and photoluminescence spectra before and after irradiations for samples SIC-T16 and BTCP-2467, respectively. Within the measurement errors the

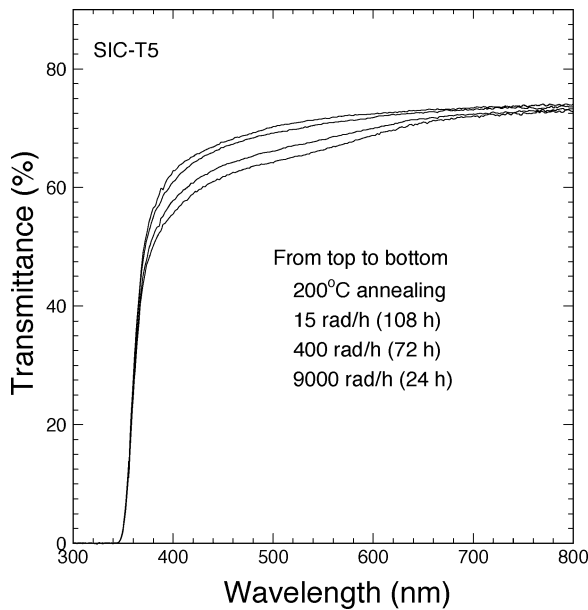


Fig. 10. Longitudinal transmittance is shown as a function of wavelength for sample SIC-T5 before and after irradiations in equilibrium at different dose rates.

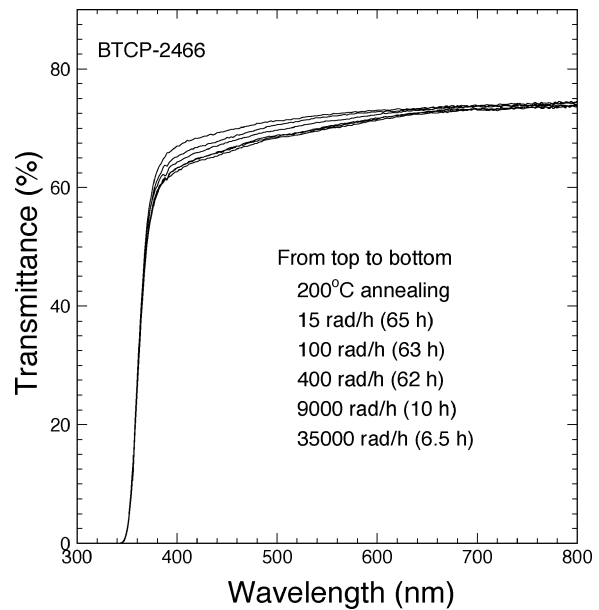


Fig. 11. Longitudinal transmittance is shown as a function of wavelength for sample BTCP-2466 before and after irradiations in equilibrium at different dose rates.

shape of these spectra are identical, indicating that the scintillation mechanism in PWO crystals is not damaged by the γ -ray irradiations.

Although there is no damage to the scintillation mechanism, color centers are created during irradiations, which absorb scintillation light, and thus reduce the measured light output. It is known that radiation induced color centers may annihilate in room temperature. During irradiation, both annihilation and creation processes coexist, the color center density reaches an equilibrium at a level depending on the dose rate applied. Assuming the annihilation speed of the color center i is proportional to a constant a_i and its creation speed is proportional to a constant b_i and the dose rate (R), the differential variation of color center density when both processes coexist can be written as [7]

$$dD = \sum_{i=1}^n \{-a_i D_i + (D_i^{all} - D_i) b_i R\} dt \quad (1)$$

where D_i is the density of the color center i in the crystal and the summation goes through all centers. The solution of (1) is

$$D = \sum_{i=1}^n \left\{ \frac{b_i R D_i^{all}}{a_i + b_i R} \left[1 - e^{-(a_i + b_i R)t} \right] + D_i^0 e^{-(a_i + b_i R)t} \right\} \quad (2)$$

where D_i^{all} is the total density of the trap related to the center i and D_i^0 is its initial density. The color center density in equilibrium (D_{eq}) depends on the dose rate (R) applied

$$D_{eq} = \sum_{i=1}^n \frac{b_i R D_i^{all}}{a_i + b_i R}. \quad (3)$$

Figs. 10 and 11 show longitudinal transmittance as a function of wavelength measured before and after a series of irradiations for samples SIC-T5 and BTCP-2466, respectively. The curves

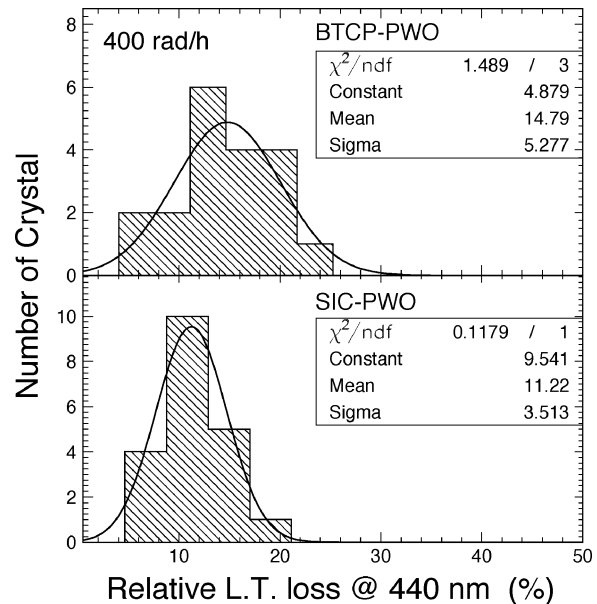


Fig. 12. A comparison of 440 nm longitudinal transmittance degradation in equilibrium at 15 rad/h.

in each plot, in order from top to bottom, represent the transmittance before irradiation and when they reached an equilibrium under a specified dose rate. Fig. 12 compares the amplitudes of degradation of the normalized transmittance at 440 nm in an equilibrium at a dose rate of 15 rad/h. The average loss of transmittance at 440 nm are 15% and 11% with normalized rms spreads of 36% and 31% for samples from BTCP and SIC respectively.

Figs. 13 and 14 show the measured light output normalized to that before irradiation (solid dots with error bars) as a function of time under irradiations for SIC and BTCP samples. Measurements were done step by step for different dose rates: 15, 100, and 400 rad/h, as shown in these figures. The degradation of the

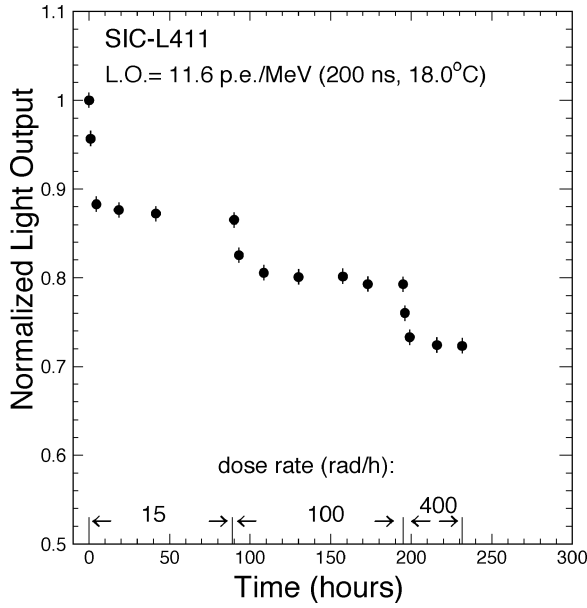


Fig. 13. Normalized light output is shown as a function of time under irradiations for a sample SIC-L411.

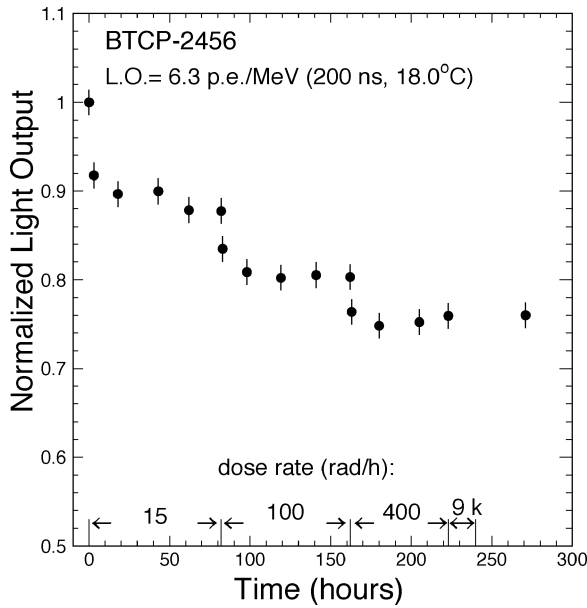


Fig. 14. Normalized light output is shown as a function of time under irradiations for a sample BTCP-2456.

light output shows a clear dose rate dependence. At the maximum dose rate expected by the CMS barrel calorimeter at LHC (15 rad/h), the loss of the light output is about 5% to 15%.

Fig. 15 compares the amplitudes of degradation in normalized light output in equilibrium at a dose rate of 15 rad/h. The average loss of light output is 17% and 12% with normalized rms spreads of 38% and 21% for samples from BTCP and SIC, respectively.

There is, however, a strong correlation between variations of the light output and the transmittance, which is the foundation of light monitoring for a precision crystal calorimeter [10], [11]. Since longitudinal transmittance can be measured to 0.2% precision, which is much better than the precision achievable for the light output measurement, the amplitude of the emission weighted radiation induced absorption coefficient ($EWRIAC$)

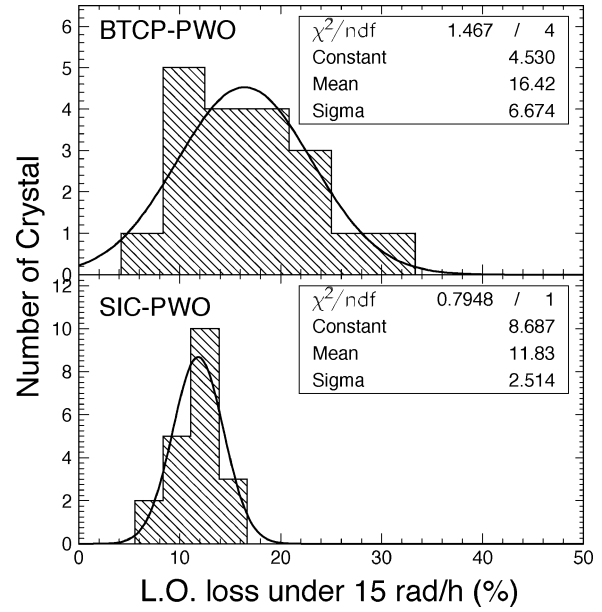


Fig. 15. A comparison of light output degradation in equilibrium at 15 rad/h.

can be used to evaluate the loss of light output, and is a good measure of radiation hardness. The $EWRIAC$ is defined as

$$EWRIAC = \frac{\int Ri_{ac}(\lambda)Em(\lambda)d\lambda}{\int Em(\lambda)d\lambda} \quad (4)$$

where $Ri_{ac}(\lambda)$ is the radiation induced absorption coefficient or color center density, and $Em(\lambda)$ is the intensity of the scintillation emission. The inverse of the $EWRIAC$ can be seen as the degraded light attenuation length. The radiation induced absorption coefficient (Ri_{ac}), or color center density, were calculated according to an equation

$$Ri_{ac} = \frac{1}{LAL_{equilibrium}} - \frac{1}{LAL_{before}} \quad (5)$$

where the subscripts “equilibrium” and “before” refer to “in equilibrium” and “before irradiation” respectively. The LAL is the light attenuation length calculated by using the longitudinal transmittance according to

$$LAL = \frac{\ell}{\ln \left\{ \frac{[T(1-T_s)^2]}{[\sqrt{4T_s^4 + T^2(1-T_s^2)^2} - 2T_s^2]} \right\}} \quad (6)$$

where T is the transmittance measured along crystal length ℓ and T_s is the theoretical transmittance without internal absorption

$$T_s = (1 - R)^2 + R^2(1 - R)^2 + \dots = \frac{(1 - R)}{(1 + R)} \quad (7)$$

and

$$R = \frac{(n_{crystal} - n_{air})^2}{(n_{crystal} + n_{air})^2}. \quad (8)$$

Figs. 16 and 17 show distributions of the $EWRIAC$ as function of the γ -ray dose rate for samples from SIC and BTCP respectively. Table I lists numerical values of the average and normalized rms of some measured optical and scintillation proper-

TABLE I
AVERAGE AND NORMALIZED RMS (IN BRACKETS) OF OPTICAL AND SCINTILLATION PROPERTIES

| PWO Vendor | ILT [†] @440 nm (%) | ILO [†] (p.e./MeV) | ILO [†] Fraction (%) | | Δ LO ^{†‡} (%) | <i>EWRIAC</i> (m ⁻¹) | | |
|------------|------------------------------|-----------------------------|---------------------------------------|--|-------------------------------|----------------------------------|------------|-------------|
| | | | $\frac{50 \text{ ns}}{1 \mu\text{s}}$ | $\frac{100 \text{ ns}}{1 \mu\text{s}}$ | | 15 rad/h | 400 rad/h | 9,000 rad/h |
| BTCP | 69.8 (1.4%) | 6.4 (12%) | 81.8 (4.0%) | 95.8 (1.6%) | 16.9 (38%) | 0.16 (45%) | 0.69 (37%) | 1.43 (50%) |
| SIC | 65.6 (1.5%) | 10.1 (9.6%) | 83.9 (4.1%) | 95.9 (1.9%) | 11.7 (20%) | 0.10 (33%) | 0.51 (32%) | 1.16 (48%) |

[†] ILT, ILO and LO stands for initial longitudinal transmittance, initial light output and light output, respectively.

[‡] Measured in equilibrium under 15 rad/h.

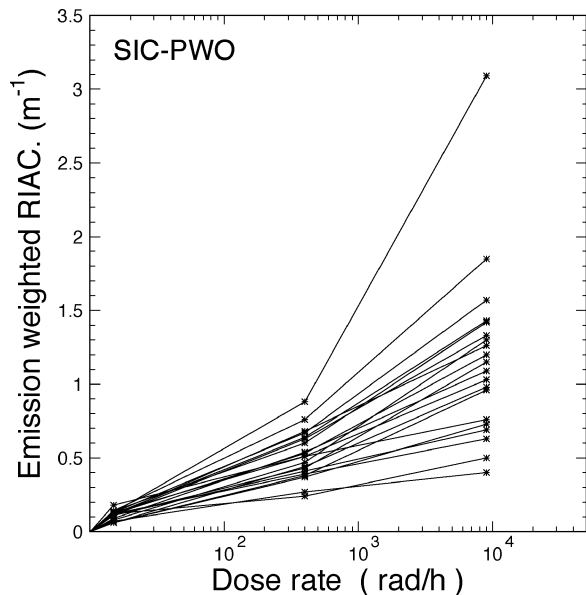


Fig. 16. The *EWRIAC* is shown as function of dose rate for SIC samples.

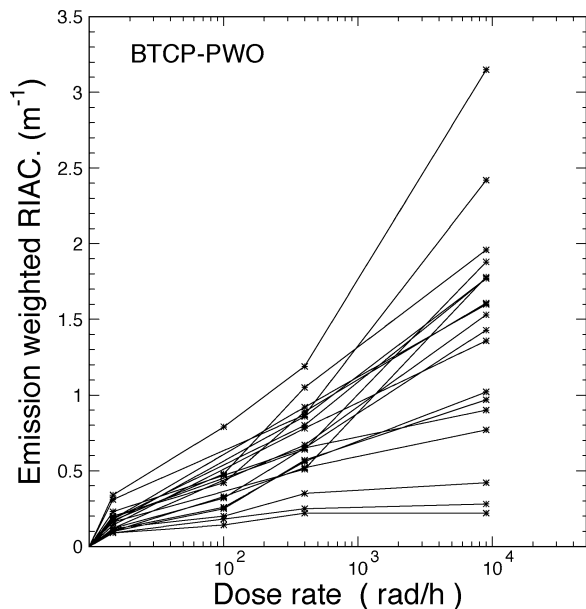


Fig. 17. The *EWRIAC* is shown as function of dose rate for BTCP samples.

ties. PWO samples produced at SIC are less divergent than that from BTCP, which may be explained by the modified Bridgman growth technology used at SIC.

While variations of the amplitude of the light output can be inter-calibrated, the loss of the energy resolution, caused by the

degradation of light response uniformity is not recoverable [7]. It is known that the shape of light response uniformity curves does not change if the degraded light attenuation length is longer than five times crystal length, or 1 m in this case [7]. If so, there will be no degradation in calorimeter energy resolution. Requiring $EWRIAC \leq 1 \text{ m}^{-1}$, currently mass produced PWO crystals may be used to build a precision crystal calorimeter in a radiation environment where the dose rate is up to a few hundred rad/h. We plan to further study the difference of PWO crystals with different radiation hardness, and to develop crystals to be used in a severe radiation environment, such as SLHC, where a dose rate of up to 10 000 rad/h is expected.

It is, however, unfortunate that no correlation was observed between the initial transmittance, or any other optical parameter, and crystal's radiation hardness. This means that the only effective approach to evaluate a PWO crystal's radiation hardness is to measure it under irradiation.

IV. SUMMARY

After extensive R&D in the past decade, mass production capabilities are now established for PWO crystals. Crystals produced in both BTCP and SIC are of good quality, sufficient to be used in a radiation environment of a dose rate up to a few hundred rad/h. Advanced R&D, however, is needed to understand and develop PWO crystals to be used in a radiation environment of higher dose rate, such as Super LHC, where dose rate of up to 10 000 rad/h is expected [12].

ACKNOWLEDGMENT

The authors thank CMS ECAL Collaboration for providing the BTCP samples used in this study. They also thank J. Y. Liao, D. S. Yan, P. Z. Yang, and Z. W. Yin for providing samples from SIC.

REFERENCES

- [1] X. D. Qu, L. Y. Zhang, R. Y. Zhu, J. Y. Liao, D. Z. Shen, and Z. W. Yin, "A study on yttrium doping in lead tungstate crystals," *Nucl. Instrum. Methods*, vol. A480, pp. 470–487, 2002.
- [2] E. Auffray, F. Cavallari, P. Lecoq, P. Sempere, and M. Schneegans, "Status of the PWO crystal production from Russia for CMS-ECAL," *Nucl. Instrum. Methods*, vol. A486, pp. 111–115, 2002.
- [3] A. Gasparian, "Performance of PWO crystal detectors for a high resolution hybrid electromagnetic calorimeter at Jefferson lab," in *Proc. 10th Int. Conf. Calorimetry in Particle Physics*, R. Y. Zhu, Ed., 2002, pp. 208–214.
- [4] R. Y. Zhu. (2003, Dec.) A study on type III samples. [Online] Available: http://www.hep.caltech.edu/zhu/ryz_031209_pwo.pdf
- [5] R. Y. Zhu, D. A. Ma, H. B. Newman, C. L. Woody, J. A. Kierstead, and S. B. Paul, "A study on properties of lead tungstate crystals," *Nucl. Instrum. Methods*, vol. A376, pp. 319–334, 1996.

- [6] R. Y. Zhu, Q. Deng, H. Newman, C. L. Woody, J. A. Kierstead, and S. B. Paul, "A study on radiation hardness of lead tungstate crystals," *IEEE Trans. Nucl. Sci.*, vol. 45, pp. 686–691, June 1998.
- [7] R. Y. Zhu, "Radiation damage in scintillating crystals," *Nucl. Instrum. Methods*, vol. A413, pp. 297–311, 1998.
- [8] G. F. Bakhshieva and A. M. Morozov, "Refractive-indexes of molybdate and tungstate single-crystals having scheelite structure," *Sov. J. Opt. Technol.*, vol. 44, no. 9, pp. 542–543, 1977.
- [9] S. Baccaro, L. M. Barone, B. Borgia, F. Castelli, F. Cavallari, and I. Dafinei *et al.*, "Ordinary and extraordinary complex refractive index of the lead tungstate (PbWO_4) crystal," *Nucl. Instrum. Methods*, vol. A385, pp. 209–214, 1997.
- [10] X. D. Qu, L. Y. Zhang, and R. Y. Zhu, "Radiation induced color centers and light monitoring for lead tungstate crystals," *IEEE Trans. Nucl. Sci.*, vol. 47, pp. 1741–1747, Dec. 2000.
- [11] L. Y. Zhang, K. J. Zhu, R. Y. Zhu, and D. T. Liu, "Monitoring light source for CMS lead tungstate crystal calorimeter at LHC," *IEEE Trans. Nucl. Sci.*, vol. 48, pp. 372–378, June 2001.
- [12] F. Gianotti, M. L. Mangano, T. Virdee, S. Abdullin, G. Azuelos, and A. Ball *et al.*, "Physics Potential and Experimental Challenges of the LHC Luminosity Upgrade," hep-ph/0204087.